Time and temperature dependence of optical linewidths in glasses at low temperature: Spectral diffusion

R. J. Silbey, J. M. A. Koedijk, and S. Völker

Citation: J. Chem. Phys. **105**, 901 (1996); doi: 10.1063/1.471969
View online: http://dx.doi.org/10.1063/1.471969
View Table of Contents: http://jcp.aip.org/resource/1/JCPSA6/v105/i3
Published by the American Institute of Physics.

Time and temperature dependence of optical linewidths in glasses at low temperature: Spectral diffusion

R. J. Silbey
Department of Chemistry, Massachusetts Institute of Technology, Cambridge, Massachusetts 02139

J. M. A. Koedijk and S. Völker
Huygens and Gorlaeus Laboratories, University of Leiden, Leiden, The Netherlands

(Received 25 January 1996; accepted 25 March 1996)

The standard theoretical model of two-level systems in low-temperature glasses is modified so that the temperature dependence of the effective homogeneous optical linewidth is in agreement with experiment. This alters the time dependence of the width due to spectral diffusion. The new results fit recent experiments without the need for gaps in the distribution function of flip rates of the two-level-systems or the addition of extra distribution functions. © *1996 American Institute of Physics.* [S0021-9606(96)00725-8]

I. INTRODUCTION

It is now well established that low energy excitations in glasses [called two-level systems (TLS)] are responsible for the anomalous temperature dependence of the specific heat and thermal conductivity.[1–4] These TLS also cause time dependence in a number of properties,[5–10] in particular the optical linewidth (or relaxation rate) of guest chromophores in the glass, measured by hole-burning or photon-echo decay experiments. Recent experimental results[11–15] have shown that the time dependence of the spectral width or relaxation rate is approximately proportional to $\log(t_d)$, where t_d is the waiting or delay time between burning and probing the hole or between the second and third pulse in a three-pulse photon-echo experiment. This behavior agrees with the predictions of the standard model of TLS. However, there are inconsistencies between the predictions of that model and experiment; for example, some three-pulse photon-echo experiments have been fitted by assuming gaps in the relevant TLS relaxation rate distribution,[12] while some hole-burning experiments have been fitted with composite distribution functions.[13] In addition, the standard model[1,2] predicts that, at low T, the specific heat varies linearly with temperature and the thermal conductivity varies as T^2, but it is found experimentally[3,4] that many glasses have specific heats that vary as $T^{1+\gamma}$ with $\gamma\sim 0.0$–0.3 and thermal conductivities that vary as $T^{2-\delta}$ with $\delta\sim 0.1$–0.2. Finally, optical linewidths in organic glasses have been found to vary as $T^{1.3\pm 0.1}$ at low temperature,[14–16] independent of experimental time scale,[14,15] again in disagreement with the standard model.

Other evidence also indicates the need to correct the standard model: from simulations of double-well potentials and TLS in glasses,[17] distributions are found which are slightly different from those of the standard model which, when used to compute the temperature dependence of the specific heat and thermal conductivity, improve the agreement between experiment and theory.

In the present paper, we investigate the consequences of the changes in the standard model necessary to make the theory and optical experiments agree, and predict a modified time dependence of the linewidths.

The paper is laid out as follows: in Sec. II, we present the standard model; in Sec. III, we present the new model and the consequences for the experiment; in Sec. IV, we compare the predictions of the new model with recent experimental data, and in Sec. V we conclude. The mathematical details are relegated to the Appendix in order not to obscure the basic ideas.

II. THE STANDARD MODEL

In a glass, there will be many double-well potentials with minima representing two stable configurations of the molecules making up the glass. Some of these double-well potentials will be approximately symmetric, producing two nearly degenerate energy states (one on the left and one on the right of the double-well potential) separated in energy by ϵ. There will also be a tunneling matrix element between the two states represented by Δ. Such a double well potential can be represented as a two-level system (TLS). Thus each TLS is determined by two parameters, ϵ and Δ. Since the glass is an amorphous material, these two parameters are distributed with a joint probability distribution $P(\epsilon,\Delta)$. The first assumption of the standard model is that ϵ and Δ are uncorrelated, so that $P(\epsilon,\Delta)$ is the product of *independent* probability distributions $P_\epsilon(\epsilon)$ and $P_\Delta(\Delta)$ that have the following forms:[1,2]

$$P_\epsilon(\epsilon)=\text{constant}\quad [|\epsilon|<\epsilon_{\max}], \tag{1}$$

$$P_\Delta(\Delta)\sim 1/\Delta\quad [\Delta_{\min}<\Delta<\Delta_{\max}]. \tag{2}$$

Equation (1) is based on: (a) the distribution must be even in ϵ, since $+\epsilon$ and $-\epsilon$ must be equally likely, and (b) a lack of any experimental or theoretical reasons to assume a specific functional form for the distribution function. Equation (2) is based on the usual Wentzel–Kramers–Brillouin (WKB) picture for the tunneling matrix element[18] that $\Delta\sim\exp(-\lambda)$, where λ is the WKB integral from left to right in the double well. Since there was no experimental or theoretical reason for there to be structure in the distribution in λ, $P_\lambda(\lambda)$, the

standard model assumes that it is constant between some minimum and maximum λ. Equation (2) follows from $P_\Delta(\Delta)=P_\lambda(\lambda)|d\lambda/d\Delta|=\text{constant}/\Delta$. Thus the distribution functions of Eqs. (1) and (2) are reasonable guesses, without foundation from more basic theory. Other assumptions of the model are that $kT \ll \epsilon_{\max}$ and that the range of Δ is in general very large (i.e., over more than 5 or 6 orders of magnitude).

When Eqs. (1) and (2) are used in the standard statistical mechanical equations for the specific heat (C) and thermal conductivity (κ) at low temperatures, it is found that

$$C \sim T, \tag{3}$$

$$\kappa \sim T^2, \tag{4}$$

agreeing qualitatively with the experimental results. A few years after the original papers of Anderson *et al.*[1] and Phillips,[2] Black and Halperin[5] derived the consequences of these distributions for spectral diffusion. Although the derivation was for phonon echo decays, it is valid for spectral diffusion of optical linewidths and photon-echo decays as well. Their calculation shows that the distribution in ϵ and Δ leads to a broad distribution in relaxation or flip rates of the TLS. Thus some TLS relax quickly, while others relax much more slowly. This gives rise to spectral diffusion of the chromophore transition energy causing a broadening of the optical line. In later papers, Hu and Walker[6] and Maynard *et al.*[7] discussed spectral diffusion in terms of the standard model. Recently, Huber[8] and Suarez and Silbey[10] theoretically extended the earlier work (to include more general TLS-phonon interactions and different averaging techniques), and Bai and Fayer[9] discussed the connection between hole-burning and photon-echo decay experiments and spectral diffusion. The predictions of all these papers is that spectral diffusion results in a linewidth or a photon-echo decay time that varies *linearly* with $\log(t_d)$, where t_d is the waiting time between burning and probing a hole or between the second and third pulse in a photon-echo experiment. The log behavior is characteristic of spectral diffusion.

In order to understand the $\log(t_d)$ dependence and the new model to be presented in the next section, we will derive the distribution of relaxation or flip rates of TLS, which occurs because of interactions with phonons. After the TLS Hamiltonian is diagonalized, the transition matrix element between the two delocalized eigenstates is a function of phonon coordinate. Thus, phonons can excite or de-excite the TLS eigenstates. The standard golden rule formula then leads to a rate, R, of TLS population relaxation which is the sum of the excitation and de-excitation rates given by[19]

$$\begin{aligned} R &= [\gamma^2/2\pi h^4 \rho v^5]\Delta^2 E \coth[E/2kT] \\ &= c\Delta^2 E \coth[E/2kT], \end{aligned} \tag{5}$$

where γ is the deformation potential parameter, ρ is the density of the glass, v is the sound velocity, E is the energy difference between the eigenstates in the double well, $E = \{\epsilon^2 + \Delta^2\}^{1/2}$ and k is the Boltzmann constant. The probability distribution of R due to the distribution of Δ and ϵ may now be calculated for a given E, by summing all ϵ and Δ that are consistent with a given R and E [see the Appendix (part 1) where it is derived for more general forms of the distribution functions]:

$$\begin{aligned} P(R,E) &= \int d\epsilon \int d\Delta\ \delta\{R - c\Delta^2 E \coth[E/2kT]\} \\ &\quad \times \delta\{E - \{\epsilon^2+\Delta^2\}^{1/2}\} P(\epsilon) P(\Delta) \end{aligned} \tag{6}$$

$$\sim \frac{1}{R\{1 - R/R_{\max}(E)\}^{1/2}}, \tag{7}$$

where $R_{\max}(E) = cE^3 \coth[E/2kT]$ is the maximum rate for a TLS with energy level separation E. Note that $P(R,E)$ increases very rapidly near $R = 0$; this produces the wide distribution of relaxation rates and the spectral diffusion at long times.

The calculation of the spectral diffusion from $P(R,E)$ was first presented by Black and Halperin[5] following the earlier work by Klauder *et al.*[20] on spectral diffusion in magnetic resonance. These authors[5] show that the linewidth related to ''pure dephasing'' and three-pulse photon-echo decay rate varies with the delay or waiting time, t_d, as

$$\begin{aligned} &[1/(\pi T_2^*)]_{\mathrm{SD}}(t_d) \\ &\quad \sim \int_0^{E_{\max}} dE\ \operatorname{sech}^2[E/2kT] \int_{R_{\min}}^{R_{\max}} dR\ P(R,E) \\ &\quad \times [1 - e^{-R} t_d]. \end{aligned} \tag{8}$$

For R's such that $Rt_d \ll 1$, the term $[1 - e^{-R}t_d]$ is small. Thus the integral is dominated by large Rt_d. We can therefore replace the lower limit by $1/t_d$ if $1/t_d > R_{\min}$ and neglect the exponential to find

$$\begin{aligned} &[1/(\pi T_2^*)(t_d)]_{\mathrm{SD}} \\ &\quad \sim \int_0^{E_{\max}} dE\ \operatorname{sech}^2[E/2kT] \int_{t_d^{-1}}^{R_{\max}} dR\ P(R,E) \\ &\quad = kT \int_0^{E_{\max}/kT} dx\ \operatorname{sech}^2[x/2] \int_{(R_{\max} t_d)^{-1}}^{1} dz \frac{1}{z} \end{aligned} \tag{9}$$

$$\sim T \ln[t_d], \tag{10}$$

where the substitutions $x = E/kT$ and $z = R/R_{\max}(E)$ have been made.

Other theoretical evaluations[6–10] of $1/\pi T_2^*(t_d)$ using slightly different expressions and mathematical analyses yield the same final form. Thus, the standard model predicts that the linewidth increases linearly with temperature and linearly with the logarithm of time. This temperature dependence is in disagreement with much of the experimental data in organic glasses which indicate at $T^{1.3}$ dependence. In order to reproduce this, we can insert a distribution in E in the integral of Eq. (9) in an *ad hoc* manner in order to obtain the $T^{1.3}$ dependence. However, as we can see from the above derivation, the T dependence and the time dependence are intertwined and arise from the assumed form of the distribution functions in ϵ and Δ, and not just the distribution function in E. In other words, a modification of the distribution

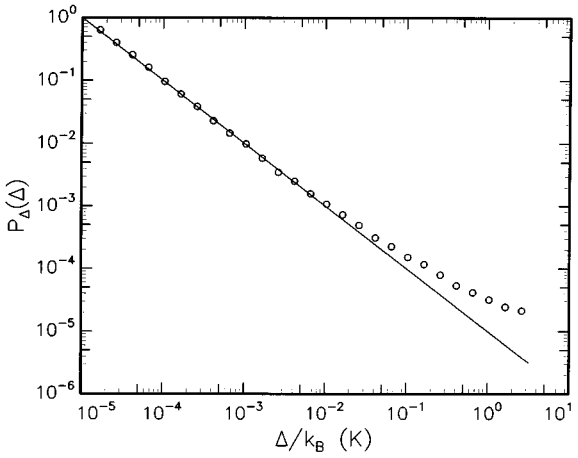

FIG. 1. Distribution of $P_\Delta(\Delta)$ as derived by Heuer and Silbey (Ref. 17). The straight line is the prediction of the standard tunneling model (STM), $P_\Delta(\Delta) = 1/\Delta$. The open circles are the results of the simulations in Ref. 17. $P_\Delta(\Delta)$ has been normalized so that $P_\Delta(\Delta/k_B = 10^{-5}\ \mathrm{K})=1$.

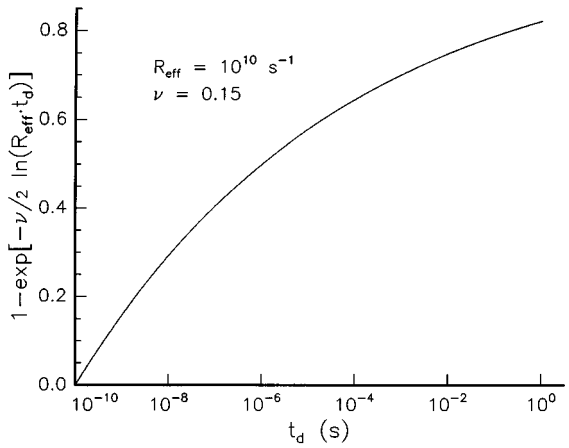

FIG. 2. The waiting time (t_d) dependence of $1/(\pi T_2^*)$ as given in Eq. (16), for $R_{\mathrm{eff}} = 10^{10}\ \mathrm{s}^{-1}$ and $\nu=0.15$.

functions in Δ and ϵ will affect the rate distribution $P(R,E)$ in more than just its temperature dependence. Therefore, if we modify the standard model to obtain the correct temperature dependence, we must reconsider the time dependence of the linewidth as well.

There is other evidence that the distribution function in Δ should be modified. In recent simulations of the configurations of glasses by Heuer and Silbey,[17] the distribution functions of the tunneling matrix element $P_\Delta(\Delta)$ and energy asymmetry $P_\epsilon(\epsilon)$ were numerically determined. These authors studied a particular glass (Ni–P at a given composition) and found that, to the accuracy of their calculation, $P_\epsilon(\epsilon)$ was constant, but $P_\Delta(\Delta)$ *differed* from the standard model. Their distribution function is shown in Fig. 1. Note that $P_\Delta(\Delta) \sim 1/\Delta$ (as in the standard model) for Δ/k_B less than $\sim 10^{-3}$ K, but as Δ increases, $P_\Delta(\Delta)$ is best fitted by a form $1/\Delta^{1-\nu}$ where ν increases to $\sim$0.2 as Δ/k_B increases beyond 1 K. Although these results are not quantitatively accurate for all glasses, they do indicate that it may be necessary to change the assumptions of the standard model. Heuer and Silbey[17] showed that with the new distribution functions the temperature dependence of the specific heat and thermal conductivity were in better agreement with experiment.

III. NEW MODEL

In this section, we modify the standard model by changing the form of the distribution functions given in Eqs. (1) and (2) so that the temperature dependence mentioned above is in accord with experiment. We then determine the waiting time dependence of $(\pi T_2^*)^{-1}$ based on these modifications.

We replace the probability distributions in Eqs. (1) and (2) by

$$P(\epsilon)\sim|\epsilon|^{\mu}, \tag{11}$$

$$P(\Delta)\sim 1/\Delta^{1-\nu}. \tag{12}$$

This leads to $C \sim T^{1+\mu+\nu}$, $\kappa \sim T^{2-\mu-\nu}$ and spectral widths $\sim T^{1+\mu+\nu}$. The rate distribution, Eq. (7), becomes (see Appendix A)

$$P(R,E)\sim \frac{E^{\mu+\nu}}{R^{1-\nu/2}[1-R/R_{\max}(E)]^{(1-\mu)/2}} \tag{13}$$

and the linewidth or relaxation rate, Eq. (10) becomes

$$[1/(\pi T_2^*)(t_d)]_{\mathrm{SD}} \sim \int_0^{E_{\max}} dE\ \mathrm{sech}^2[E/2kT]\int_{t_d^{-1}}^{R_{\max}} dR\ P(R,E) \tag{14}$$

$$\sim (2/\nu)T^{\mu+\nu+1}[1-(R_{\mathrm{eff}}\ t_d)^{-\nu/2}] \tag{15}$$

or

$$[1/(\pi T_2^*)(t_d)]_{\mathrm{SD}} = aT^{\mu+\nu+1}[1-\exp-\{\nu/2\ \ln(R_{\mathrm{eff}}\ t_d)\}], \tag{16}$$

where R_{eff} is an effective maximum rate averaged over the energy distribution and a is a collection of constants (proportional to $1/\nu$) and interaction strengths [see Eq. (A12)]. Note that in the limit $\nu\to 0$, the linewidth is linear in $\ln(t_d)$ agreeing with the standard model.

Thus, changing the distribution functions in ϵ and Δ to yield a nonlinear T dependence produces a nonlinear dependence in $\ln(t_d)$ for the broadening of the width due to spectral diffusion. Another prediction is that the two-pulse photon-echo decay will not be strictly exponential in τ (the time between the first two $\pi/2$ pulses), but will vary as $\exp[-\tau^{1-\nu/2}]$. From fitting various experimental data in the literature (Sec. IV), we find ν to be on the order of 0.00–0.15, so that the nonexponentiality is small and probably unobservable. However, as we will see, the effect of the change in the distribution functions is observable in the spectral diffusion because of the many orders of magnitude in waiting time that are possible in the experiment.

In Fig. 2, the t_d dependent part of the linewidth is plotted for ν=0.15 and $R_{m,\mathrm{eff}} = 10^{10}\ \mathrm{s}^{-1}$. Note that for four or five orders of magnitude in time, the curve can be fitted reason-

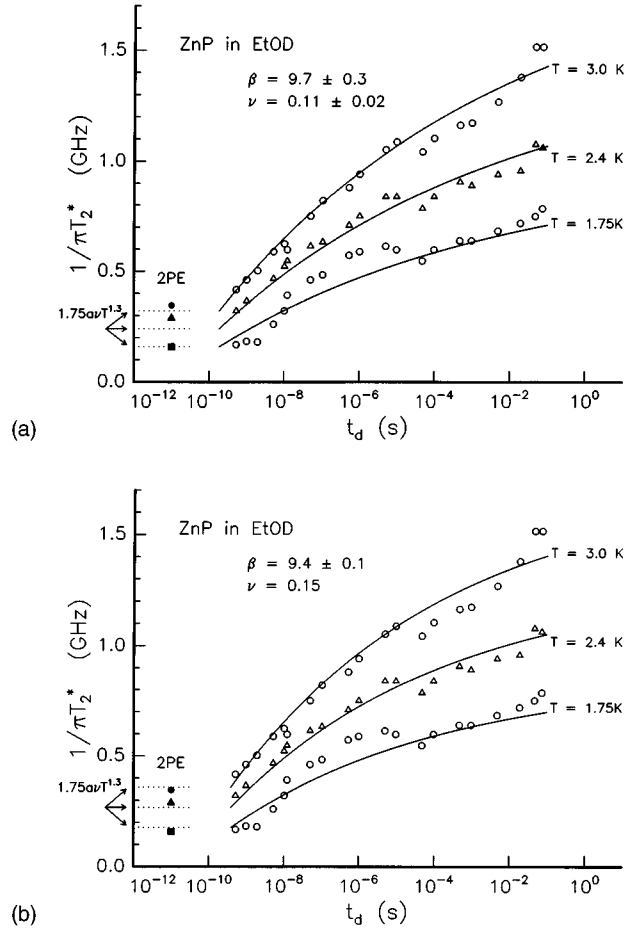

FIG. 3. (a) Three-pulse photon-echo decay rates as a function of delay t_d for zinc porphin in deuterated ethanol at three temperatures, from Ref. 12(c). The solid lines are a fit of Eq. (19) to the data. Both β and ν are allowed to vary. The best values are given in the figure. The values of the two-pulse photon-echo decay rates are also given in the figure (filled squares) along with the prediction of the model (dotted lines). (b) Same as (a) but with the value of ν fixed to be equal to 0.15 and β allowed to vary.

ably well with a linear function of $\ln(t_d)$. However, if one looks over seven or more orders of magnitude in time, the curvature is evident.

In the Appendix (part 3), we calculate the decay rate arising from spectral diffusion that contributes to the two-pulse photon-echo decay (and short-time linewidth). We find, for ν between 0.0 and 0.25,

$$[1/\pi T_2^*]_{2\mathrm{PE}} \cong (1.75 \pm 0.1) a\ \nu\ T^{\mu+\nu+1}. \tag{17}$$

In the next section we will compare the calculated linewidth or decay rate with the data of various experimental groups.

IV. COMPARISON TO EXPERIMENT

The effective homogeneous linewidth Γ'_{hom} is given by $1/(2\pi T_1) + 1/(\pi T_2^*) = \Gamma_0 + (1/\pi T_2^*)$, where T_1 is the fluorescence lifetime of the excited state. The value of $[1/\pi T_2^*]$ is given by the sum of Eqs. (16) and (17):

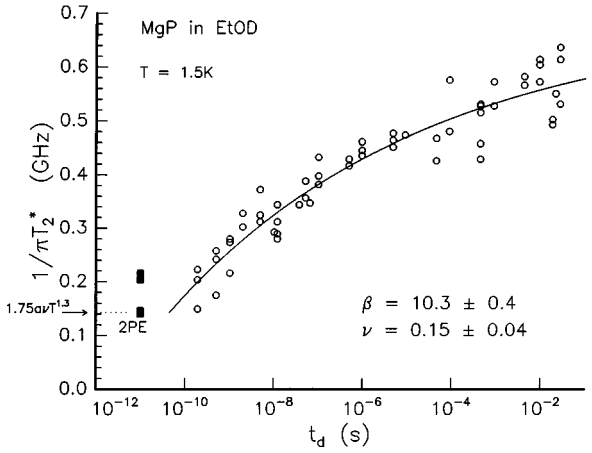

FIG. 4. Three-pulse photon-echo decay rates for magnesium porphin [MgP] in deuterated ethanol [EtOD] at 1.5 K (open circles) from Ref. 12(b) and 12(c). The solid line is a fit of Eq. (19) to the data. The best values of β and ν are given in the figure. The values of the two-pulse photon-echo decay rates are also given in the figure (filled squares) along with the prediction of the model (dotted line).

$$[1/\pi T_2^*] = 1.75\ a\ \nu\ T^{\mu+\nu+1} + a\ T^{\mu+\nu+1} \times [1 - \exp - \{\nu/2\ \ln(R_{m,\mathrm{eff}}\ t_d)\}] \tag{18}$$

or

$$[1/\pi T_2^*] = 1.75\ a\ \nu\ T^{\mu+\nu+1} + a\ T^{\mu+\nu+1} \times [1 - \exp - \alpha\{\beta + \log(t_d)\}], \tag{19}$$

where $\alpha = 2.303\ \nu/2$ and $\beta = \log(R_{m,\mathrm{eff}})$.

Meijers and Wiersma[12(a)–12(c)] have studied the three-pulse photon-echo decay of various chromophores in a number of glasses. In order to fit their data using the standard model, they were forced to insert a gap in the distribution of TLS flip rates. So, for example, they assumed that, for the chromophore Zn porphin in deuterated ethanol (ZnP/EtOD), there were no TLS flip rates between approximately 1 μs and 1 ms.[12(a)] The decay rate was assumed to be linear in $\ln(t_d)$ from the earliest times ($\sim 10^{-10}$ s) to 10^{-6} s, flat until 10^{-3} s, and then once more linear above 10^{-3} s, with the same slope as in the early time regime. Although this form fits the data, there is no explanation of the gap, and in addition, no explanation why the slow and fast flip regimes (below and above the gap) should have the same slope.

In Figs. 3(a) and 3(b) we show the data for ZnP/EtOD at three temperatures, taken from the thesis of Meijers,[12(c)] with two fits using the present model, Eq. (19). Figure 3(a) is a fit in which both β and ν are allowed to vary, while in Fig. 3(b), ν was fixed at 0.15 and β allowed to vary. The quality of the fits are the same. Note that the same values of β and ν fit the three temperature data. The need for a gap in the distribution function has disappeared. As shown in the figures, the predicted values of the two-pulse photon-echo decay rates also agree with experiment.

In Fig. 4, we show the three-pulse photon-echo data for magnesium porphyrin in EtOD (MgP/EtOD) taken from Ref. 12(b), and the fit using the present model. The experimental

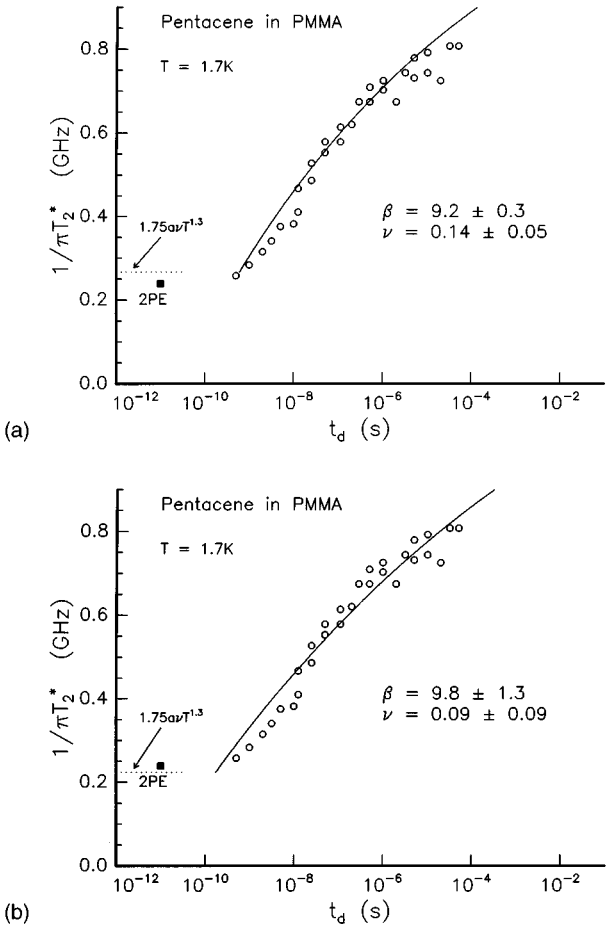

FIG. 5. (a) Three-pulse photon-echo decay rates for pentacene in PMMA at 1.7 K (open circles) from Ref. 12(b) and 12(c). The solid line is a fit of Eq. (19) to the data. The values of β and ν are given in the figure. The value of the two-pulse photon-echo decay rate is also given in the figure (filled square) along with the prediction of the model (dotted line). (b) Same as (a) but with different values of β and ν resulting from a fit to data taken over a limited time range (10^{-8} s to 10^{-4} s).

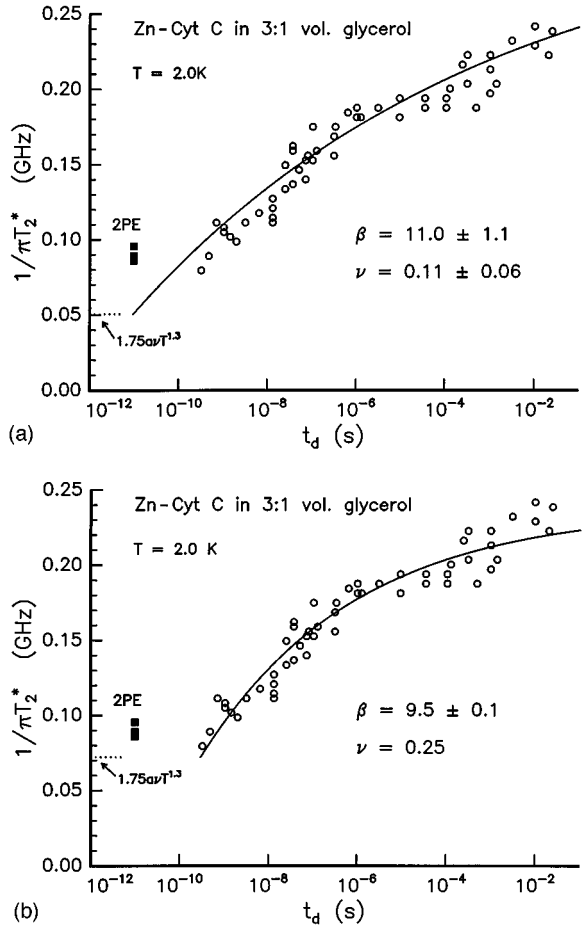

FIG. 6. (a) Three-pulse photon-echo decay rates for zinc-cytochrome c in glycerol at 2.0 K (open circles) from Ref. 12(d). The solid line is a fit of Eq. (19) to the data. The best values of β and ν are given in the figure. The values of the two-pulse photon-echo decay rates are also given in the figure (filled squares) along with the prediction of the model (dotted line). (b) Same as (a), but with the value of ν fixed at 0.25 and β allowed to vary.

uncertainty is large, especially at longer times; however, it is clear that the present model does well in fitting the data without gaps in the distribution function. The predicted two-pulse photon-echo decay rate, furthermore, agrees with experiment within the large spread in data. In addition, the values of the fitting parameters are close to those used to fit the data for ZnP/EtOD, as we might expect from the similarity of the systems and the experimental time scales.

In Figs. 5(a) and 5(b) we show the three-pulse photon-echo decay data for pentacene in PMMA[12(b)] and two fits to the data using the present model. Although the values of β differ in the two fits and the values of ν have large uncertainties, the quality of the fits are quite similar. We should remark that in the fit of Fig. 5(b), only data between 10^{-8} s and 10^{-4} s have been used. It is clear that in order to make a more precise determination of these parameters, a very large range in time is necessary.

In Fig. 6(a) the data for Zn-cytochrome-C in glycerol glass taken from Thorn Leeson and Wiersma [12*d*] are plotted along with our fit. Again, the data can be fitted with no gaps in the distribution function, and with values of β=11.0 and ν=0.11 close to those used in Figs. 3–5. However, the predicted value of the two-pulse photon-echo decay rate is much lower than the experimental value. This may indicate that there are extra dephasing processes in this system other than those described by the present model. Only with a much larger ν=0.25 and, consequently, β=9.5, the predicted two-pulse photon-echo decay rate $1.75\, a\, \nu\, T^{1.3}$ becomes closer to the experimentally obtained 2PE value, as shown in Fig. 6(b).

Next, we examine hole-burning data from two groups, and fit the values of $\Gamma'_{\rm hom} - \Gamma_0 = 1/(\pi T_2^*)$ with the present model. In Figs. 7(a) and 7(b), our results on bacteriochlorophyll-a in 2-methyltetrahydrofuran glass (BChl-a/MTHF)[15] at two temperatures are shown along with two fits to the present model. From these fits, we see that the uncertainty in the experimental data is too large to make an unambiguous determination of the values of the fitting parameters. Note that the fits are close to linear (ν=0.03 and 0.05), in contrast to the fits of the photon-echo data (ν =0.10–0.15). In Figs. 8(a) and 8(b), our data for BChl-a in

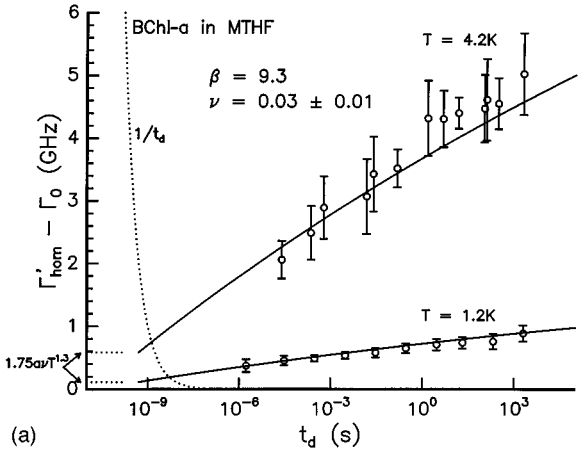

FIG. 7. (a) Effective homogeneous linewidth $\Gamma'_{\rm hom} - \Gamma_0$ (with the fluorescence lifetime contribution removed) measured by hole-burning for bacteriochlorophyll-a in MTHF at 1.2 K and 4.2 K (open circles) from Ref. 15. The solid line is a fit of Eq. (19) to the data. The value of β has been fixed to 9.3 in such a way that $10^{-\beta} < T_2^* = (\pi\ 1.75\ a\nu\ T^{1.3})^{-1}$. The value of ν follows from the fit. The predicted values of the two-pulse photon-echo decay rates are also given in the figure (dotted lines labeled 1.75 $a\ \nu\ T^{1.3}$). (b) Same as (a), but with the value of ν chosen to be maximum and such that the curve still fits the data within the error bars.

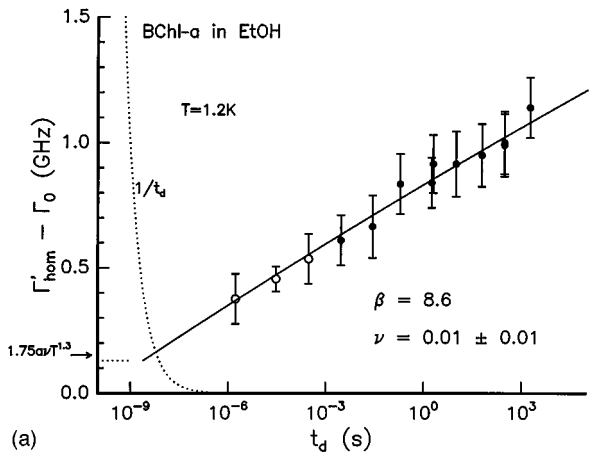

FIG. 8. (a) Effective homogeneous linewidth $\Gamma''_{\rm hom} - \Gamma_0$ (with the fluorescence lifetime contribution removed) measured by hole-burning for bacteriochlorophyll-a in ethanol at 1.2 K (open circles) from Ref. 15. The solid line is a fit of Eq. (19) to the data. The same criterion as in Fig. 7(a) was used to determine the value of β, with ν allowed to vary. The predicted value of the two-pulse photon-echo decay rate is also given in the figure (dotted line labeled 1.75 $a\ \nu\ T^{1.3}$). A good fit is obtained with β=8.6 and ν=0.01. (b) Same as (a), but with the value of ν=0.06 chosen to be maximum and such that the curve still fits the data within the error bars.

ethanol (BChl-a/EtOH)[15] at 1.2 K are shown along with two fits to the present model. We see in Fig. 8(a) that β=8.6 and ν=0.01, whereas in Fig. 8(b) we have taken the largest value of ν=0.05 that would still fit the data within the error bars. Finally, in Figs. 9(a) and 9(b), the data of Littau *et al.*[13] on the holewidths and two-pulse photon-echo decay rate of cresyl violet in deuterated ethanol (CV/EtOD) at 1.3 K are shown with two fits: β=8.8 and ν=0.005 (almost linear) in Fig. 8(a) and β=8.8 and ν=0.02 in Fig. 9(b). The predicted value of the two-pulse photon-echo decay rate in Figs. 9(a) and 9(b) coincides with the experimental one.[13] From Figs. 8 and 9, we see that the hole-burning data in ethanol from two groups can be fitted consistently.

The values of ν differ for the two kinds of experiments (hole-burning and three-pulse photon-echo). This can be explained by examining the results of the simulations of glass dynamics by Heuer and Silbey,[17] who evaluated the distribution function of tunneling rates and found that at longer times the effective ν was almost zero, while at shorter times, ν was closer to 0.2. Since the waiting times for hole-burning experiments are longer than for three-pulse photon-echo experiments, we predict that the fitted values of ν will be smaller in the former than in the latter, which is what we indeed find.

The fitted values of β for various chromophores in ethanol glass range from ~8.6 to ~10.3, an almost two orders of magnitude difference in effective maximum rate, 10^{β}. Note that the smaller values of β occur for hole-burning experiments (with waiting times longer than 10^{-6} sec), while larger values of β are found in the three-pulse photon-echo experiments (with waiting times longer than 10^{-10} sec). How do we then choose β for a particular glass? One criterion that should be met is that the effective maximum rate 10^{β} should be at least as large as $(T_2^*)^{-1}$, the value corresponding to the two-pulse photon-echo decay. If this is true, then there are fluctuations fast enough to cause short-time dephasing with-

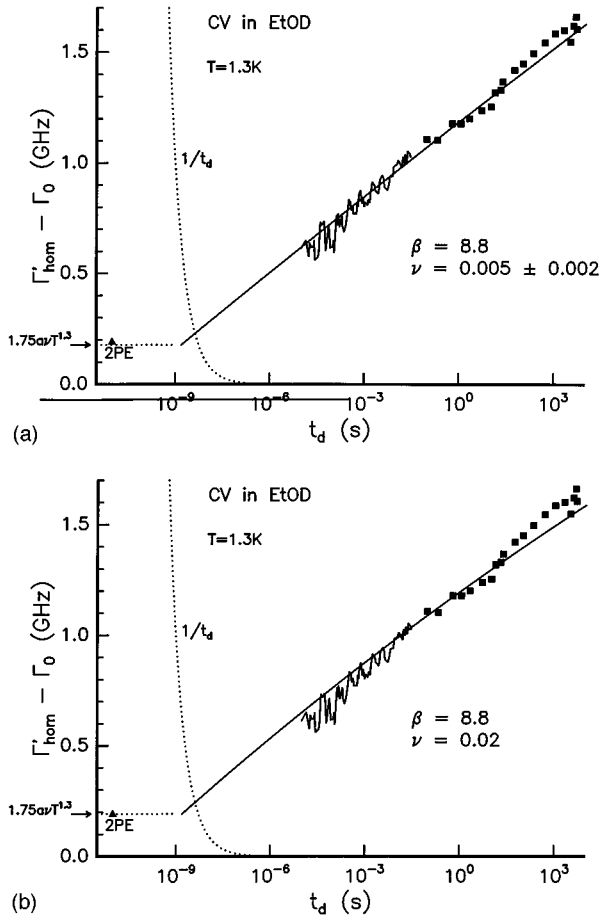

FIG. 9. (a) Effective homogeneous linewidth $\Gamma''_{\rm hom} - \Gamma_0$ (with the fluorescence lifetime contribution removed) measured by hole-burning for cresyl violet (CV) in deuterated ethanol (EtOD) at 1.3 K (filled squares and noisy line) from Ref. 13. The solid line is a fit of Eq. (19) to the data. The value of β has been determined by the same criterion as used above, $10^{-\beta} < T_2^* = (\pi\ 1.75\ a\ \nu\ T^{1.3})^{-1}$. while ν was allowed to vary. Notice that the best fit is linear ($\nu = 0.005$). The predicted value of the two-pulse photon-echo decay rate (dotted line labeled $1.75\ a\ \nu\ T^{1.3}$) coincides with the experimental value (filled triangle). (b) Same as (a), but with the value of ν=0.02 chosen to be maximum such that the curve still fits the data. Note that the parameters β and ν of both (a) and (b) agree with those of Figs. 8(a) and 8(b).

out gaps in the rate distribution. We have used this criterion in all the fits.

Both the present model and the standard model assume that fluctuations that produce the short-time dephasing and those that produce the longer time spectral diffusion arise from a single distribution of TLS-flip rates. The question is then whether a consistent set of parameters β and ν can be found for a given glass, e.g., ethanol, that describes the decay over the entire time range covered by three-pulse photon-echo- and hole-burning experiments. This problem is taken up in another publication.[15]

V. CONCLUSIONS

We have presented a calculation of the dephasing rate or linewidth due to spectral diffusion, allowing for the distribution function of flip rates, $P(R)$, to be different from that in previous models. This change in the distribution was motivated from two directions: (1) recent simulations of the TLS in low temperature glasses[17] predicted that the distribution function for fast rates would vary as $R^{-(1-\nu/2)}$ and for slow rates as R^{-1}, and (2) the necessity to reconcile theoretically the predicted linear $\ln(t_d)$ dependence with the observed $T^{1.3}$ temperature dependence of the holewidths and photon-echo data. Using the new $P(R)$, we were able to fit the experimental data quantitatively, without introducing gaps or additional functions in the rate distribution. More theory and computations have to be done to interpret all the parameters in the new model.

ACKNOWLEDGMENTS

We would like to thank J. Skinner for pointing out the range of physically acceptable values of β in Eq. (19). R.S. would like to thank the National Science Foundation, and J.K. and S.V. would like to thank the Netherlands Foundations for Physical Research (FOM) and Chemical Research (SON) and the Netherlands Organization for Scientific Research (NWO) for financial support of this work. Discussions with F. T. H. den Hartog, T. M. H. Creemers are gratefully acknowledged.

APPENDIX

1. Calculation of $P(R,E)$

From Eq. (6) the distribution function $P(R,E)$ is given by

$$P(R,E) = \int d\epsilon \int d\Delta\ \delta\{R - c\Delta^2 E\ \coth[E/2kT]\} \times \delta\{E - \{\epsilon^2+\Delta^2\}^{1/2}\} P(\epsilon) P(\Delta) \tag{A1}$$

$$= \text{constant} \int d\epsilon \int d\Delta\ \delta\{R - c\Delta^2 E \times \coth[E/2kT]\}\, \delta\{E - \{\epsilon^2+\Delta^2\}^{1/2}\}\, \epsilon^{\mu} \Delta^{\nu-1}. \tag{A2}$$

Using the identity $\delta[(x-a)(x+a)] = (x+a)^{-1}\delta(x-a)$ and making the change in variable $y = \Delta^2$, we find

$$P(R,E) = \text{constant} \int d\epsilon\ \delta\{R - R_{\max} + R_{\max}\epsilon^2/E^2\} \times (E^2-\epsilon^2)^{\nu/2} \epsilon^{\mu} \frac{E}{E^2-\epsilon^2} \tag{A3}$$

for $\Delta^2_{\min} < E^2 - \epsilon^2 < \Delta^2_{\max}$ and where $R_{\max} = cE^3 \coth(E/2kT)$. Making a further change in variable $x = \epsilon^2/E^2$, we find

$$P(R,E) = \text{constant} \int dx\ \delta\{R - R_{\max} + xR_{\max}\} \times (1-x)^{\nu/2-1} x^{(\mu-1)/2} E^{\mu+\nu}, \tag{A4}$$

so that

$$P(R,E)=\text{constant}\,\frac{E^{\mu+\nu}(R/R_{\max})^{\nu/2}}{R(1-R/R_{\max})^{(1-\mu)/2}}. \tag{A5}$$

Note that in the limit ν and $\mu\to 0$, the standard form is recovered.

2. Calculation of $[(1/\pi T_2^*)]_{SD}$

Hu and Walker[6] and Suarez and Silbey[10] have shown that the three-pulse photon-echo amplitude decays as $\exp[-F_1(\tau)-F_2(\tau,t_d)]$, where $F_1(\tau)$ is the two-pulse echo decay (or dephasing decay) and $F_2(\tau,t_d)$ is the decay that depends on the separation between the second and third pulse. The Fourier transform of this yields the effective homogeneous linewidth, Γ'_{hom}. In our model, using the probability distributions of Eqs. (11) and (12), we find that $F_1(\tau)$ varies as $\tau^{1-\nu/2}$ (where τ is the time between the first two pulses) which is very close to linear for all the fits in this paper and that $F_2(\tau)$ varies as τ. We define $F_2(\tau,t_d)=\tau/T_2^*$, and find $(1/\pi T_2^*)$ using the formula of Black and Halperin[5] (an identical result can be obtained using the formulas of Ref. 6 or 7). The spectral diffusion contribution to the homogeneous linewidth is given by $[1/(\pi T_2^*)]_{SD}$.

Substituting $P(R,E)$ into Eq. (9), we obtain

$$[(1/\pi T_2^*)]_{SD}=K\int_0^{E_{\max}} dE\ \operatorname{sech}^2[E/2kT] \times\int_{R_{\min}}^{R_{\max}} dR\,\frac{E^{\mu+\nu}(R/R_{\max})^{\nu/2}}{R(1-R/R_{\max})^{(1-\mu)/2}} \times[1-e^{-R}t_d], \tag{A6}$$

where K is proportional to the dipole-dipole interaction strength between the TLS and the chromophore. Note that the sech function provides an upper cutoff for E such that $E<\sim 4kT$. Defining $x=R/R_{\max}$,

$$[(1/\pi T_2^*)]_{SD}=K\int_0^{E_{\max}} dE\ E^{\mu+\nu}\operatorname{sech}^2[E/2kT] \times\int_{R_{\min}/R_{\max}}^{1} dx\,\frac{x^{\nu/2}}{x(1-x)^{(1-\mu)/2}} \times[1-e^{-2xR_{\max}t_d}]. \tag{A7}$$

In general, $R_{\min}/R_{\max}\ll 1$, so the lower limit can be replaced by 0 as long as $\nu>0$. The integral over x can then be done analytically:[21]

$$[1/\pi T_2^*]_{SD}=K\int_0^{E_{\max}} dE\ E^{\mu+\nu}\operatorname{sech}^2[E/2kT] \times\frac{\Gamma((1+\mu)/2)\Gamma(\nu/2)}{\Gamma((1+\mu+\nu)/2)} \times[1-M(\nu/2,(1+\mu+\nu)/2;-2R_{\max}t_d)], \tag{A8}$$

where $\Gamma(x)$ is the gamma function and $M(a,b;z)$ is the confluent hypergeometric function.[22] For $2R_{\max}t_d$ large (i.e., >10),

$$M(a,b;-2R_{\max}t_d)\sim\frac{\Gamma(b)}{\Gamma(b-a)}(2R_{\max}t_d)^{-a},$$

so that

$$[(1/\pi T_2^*)]_{SD}=K\int_0^{E_{\max}} dE\ E^{\mu+\nu}\operatorname{sech}^2[E/2kT] \times\frac{\Gamma((1+\mu)/2)\Gamma(\nu/2)}{\Gamma((1+\mu+\nu)/2)} \times\left(1-\frac{\Gamma((1+\mu+\nu)/2)}{\Gamma((1+\mu)/2)}(2R_{\max}t_d)^{-\nu/2}\right) \sim[1-(2R_{\text{eff}}t_d)^{-\nu/2}], \tag{A9}$$

where

$$(1/R_{\text{eff}})^{\nu/2}=\frac{\Gamma((1+\mu+\nu)/2)}{\Gamma((1+\mu)/2)} \times\frac{\int_0^{E_{\max}} dE\ E^{\mu+\nu}\operatorname{sech}^2(E/2kT)(1/R_{\max})^{\nu/2}}{\int_0^{E_{\max}} dE\ E^{\mu+\nu}\operatorname{sech}^2(E/2kT)}. \tag{A10}$$

Therefore, for $2R_{\max}t_d>10$,

$$[(1/\pi T_2^*)]_{SD}=aT^{1+\mu+\nu}\,[1-(2R_{\text{eff}}\,t_d)^{-\nu/2}], \tag{A11}$$

where

$$a=K\frac{\Gamma((1+\mu)/2)\Gamma(\nu/2)}{\Gamma((1+\mu+\nu)/2)} \times\int_0^{E_{\max}/kT} dx\ x^{\mu+\nu}\operatorname{sech}^2(x/2) \tag{A12}$$

[note that $\Gamma(\nu/2)$ is proportional to $1/\nu$ for small ν] and we have extracted the temperature dependence of the integral over E.

3. Calculation of $(1/\pi T_{2,2PE}^*)$

The calculation of $(1/\pi T_{2,2PE}^*)$ requires extending the formula derived by Huber[8] (originally derived by Maynard *et al.*[7]) or Suarez and Silbey[10] for $\nu\neq 0$. The two-pulse echo amplitude decays as $\exp[-F_1(\tau)]$ where (K is the same as in the above formulas)

$$F_1(\tau)=(1/2)K\int_0^{E_{\max}} dE\ E^{\mu+\nu}\operatorname{sech}^2[E/2kT] \times\int_{R_{\min}}^{R_{\max}}\frac{dRR_{\max}^{-\nu/2}}{(1-R/R_{\max})^{\mu/2}R^{2-\nu/2}}f(\xi,2R\tau), \tag{A13}$$

where $\xi=\tanh(E/2kT)$, τ is the time between the two pulses, and $f(\xi,x)$ is given as[6]

$$f(\xi,x)=2\int_0^x dx'e^{-x'}\int_0^{x'}dx''I_0(x'')I_0[\xi(x'-x'')]. \tag{A14}$$

Here $I_0(x)$ is the modified Bessel function of zeroth order. Hu and Walker[6] calculated $f(\xi,x)$ and showed graphs for various values of ξ. For small x, $f(\xi,x) \sim x^2$ independently of ξ, and $f(\xi,x) \sim x^{0.5}$ for x large (and $\xi<1$). Using these forms and numerically integrating Eq. (A3),

$$F_1(\tau)=(\tau/\pi T^*_{2,2PE})^{1-\nu/2},\ (1/\pi T^*_{2,2PE}) \cong \zeta a \nu T^{1+\mu+\nu}, \tag{A15}$$

where $\zeta=1.83$ for $\nu=0$ and ~ 1.7 for $\nu=0.25$, and a is the same factor that appears in the formula for $(1/\pi T_2^*)$.

[1] P. W. Anderson, B. I. Halperin, and C. M. Varma, Philos. Mag. **25**, 1 (1972).
[2] W. A. Phillips, J. Low Temp. Phys. **7**, 351 (1972).
[3] J. C. Lasjaunias, A. Ravex, M. Vandorpe, and S. Hunklinger, Solid State Commun. **17**, 1045 (1975).
[4] Th. Schmidt, J. Baak, D. A. van de Straat, H. B. Brom, and S. Völker, Phys. Rev. Lett. **70**, 3584 (1993); D. A. van de Straat, J. Baak, H. B. Brom, Th. Schmidt, and S. Völker, Phys. Rev. B **53**, 217 (1996).
[5] J. Black and B. I. Halperin, Phys. Rev. B **16**, 2879 (1977).
[6] P. Hu and L. R. Walker, Solid State Commun. **24**, 813 (1977); Phys. Rev. B **18**, 1300 (1978).
[7] R. Maynard, R. Rammal, and R. Suchail, J. Phys. Lett. **41**, L291 (1980).
[8] D. L. Huber, J. Lumin. **36**, 307 (1987); W. O. Putikka and D. L. Huber, Phys. Rev. B **36**, 3436 (1987).
[9] Y. S. Bai and M. D. Fayer, Chem. Phys. **128**, 135 (1988); Phys. Rev. B **39**, 11066 (1989).
[10] A. Suarez and R. Silbey, Chem. Phys. Lett. **218**, 445 (1994).
[11] W. Breinl, J. Friedrich, and D. Haarer, J. Chem. Phys. **81**, 3915 (1984).
[12] (a) H. Meijers and D. Wiersma, Phys. Rev. Lett. **68**, 381 (1992); (b) J. Chem. Phys. **101**, 6927 (1994); (c) H. Meijers, Ph.D. thesis, U. Groningen, 1994; (d) D. Thoorn Leeson and D. Wiersman, J. Phys. Chem. **98**, 3913 (1994).
[13] K. Littau, M. A. Dugan, S. Chen, and M. D. Fayer, J. Chem. Phys. **96**, 3484 (1992), and references therein.
[14] R. Wannemacher, J. M. A. Koedijk, and S. Völker, Chem. Phys. Lett. **206**, 1 (1993); J. M. A. Koedijk, T. M. H. Creemers, F. T. H. den Hartog, M. P. Bakker, and S. Völker, J. Lumin. **64**, 55 (1995); F. T. H. den Hartog, M. P. Bakker, J. M. A. Koedijk, T. M. H. Creemers, and S. Völker, *ibid.* **66-67**, 1 (1996).
[15] J. M. A. Koedijk, R. Wannemacher, R. J. Silbey, and S. Völker, J. Phys. Chem. (submitted).
[16] S. Völker, in *Relaxation Processes in Molecular Excited States*, edited by J. Fünfschilling (Kluwer, Dordrecht, 1989), pp. 113–242; Annu. Rev. Phys. Chem. **40**, 499 (1989), and references therein.
[17] A. Heuer and R. Silbey, Phys. Rev. Lett. **25**, 3911 (1993); Phys. Rev. B **49**, 1441 (1994); **53**, 609 (1996).
[18] E. Merzbacher, *Quantum Mechanics*, 2nd ed. (Wiley, New York, 1970), p. 118.
[19] J. Jäckle, Z. Phys. **257**, 212 (1972).
[20] J. Klauder and P. Anderson, Phys. Rev. **125**, 912 (1962).
[21] I. S. Gradstein and I. M. Rydzhik, *Tables of Integrals, Series, and Products* (Academic, New York, 1965), p. 318.
[22] M. Abramowitz and I. Stegun, *Handbook of Mathematical Functions* (Dover, New York, 1965).